agriculture

MDPI

Article

Transcriptomic Analysis Reveals the Mechanism of *MtLOX24* in Response to Methyl Jasmonate Stress in *Medicago truncatula*

Lei Xu [1,2,†], Yanchao Xu [2,†], Huanhuan Lv [2], Yanran Xu [2], Jiangqi Wen [3], Mingna Li [2], Junmei Kang [2], Zhipeng Liu [1], Qingchuan Yang [1,2] and Ruicai Long [2,*]

[1] State Key Laboratory of Grassland Agro-Ecosystems, Key Laboratory of Grassland Livestock Industry Innovation, Ministry of Agriculture and Rural Affairs, Engineering Research Center of Grassland Industry, Ministry of Education, College of Pastoral Agriculture Science and Technology, Lanzhou University, Lanzhou 730020, China; aeolianlei@163.com (L.X.); lzp@lzu.edu.cn (Z.L.); yangqingchuan@caas.cn (Q.Y.)
[2] Institute of Animal Sciences, Chinese Academy of Agricultural Sciences, Beijing 100193, China; xuasdfg0528@163.com (Y.X.); lvhuanhuan0331@163.com (H.L.); xuyanran115@163.com (Y.X.); limingna@caas.cn (M.L.); kangjunmei@caas.cn (J.K.)
[3] Department of Plant and Soil Sciences, Oklahoma State University, Stillwater, OK 73401, USA; jiangqi.wen@okstate.edu
* Correspondence: longruicai@caas.cn
† These authors contributed equally to this work.

Abstract: Lipoxygenase (LOX) is associated with responses to plant hormones, environmental stresses, and signaling substances. Methyl jasmonate (MeJA) treatment triggers the production of LOX, polyphenol oxidase, and protease inhibitors in various plants, producing resistance to herbivory. To examine the response of *MtLOX24* to MeJA, the phenotypic and physiological changes in *Medicago truncatula MtLOX24* overexpression and *lox* mutant plants were investigated. Additionally, wild-type R108, the *MtLOX24*-overexpressing line L4, and the mutant *lox-1* were utilized as experimental materials to characterize the differentially expressed genes (DEGs) and metabolic pathways in response to MeJA. The results indicate that after treatment with 200 μM of MeJA, the damage in the mutants *lox-1* and *lox-2* was more serious than in the overexpressing lines L4 and L6, with more significant leaf wilting, yellowing, and oxidative damage in *lox-1* and *lox-2*. Exogenous application of MeJA induced H_2O_2 production and POD activity but reduced CAT activity in the *lox* mutants. Transcriptome analysis revealed 10,238 DEGs in six libraries of normal-growing groups (cR108, cL4, and clox1) and MeJA-treated groups (R108, L4, and lox1). GO and KEGG functional enrichment analysis demonstrated that under normal growth conditions, the DEGs between the cL4 vs. cR108 and the clox-1 vs. cR108 groups were primarily enriched in signaling pathways such as plant–pathogen interactions, flavonoid biosynthesis, plant hormone signal transduction, the MAPK signaling pathway, and glutathione metabolism. The DEGs of the R108 vs. cR108 and L4 vs. cL4 groups after MeJA treatment were mainly enriched in glutathione metabolism, phenylpropanoid biosynthesis, the MAPK signaling pathway, circadian rhythm, and α-linolenic acid metabolism. Among them, under normal growth conditions, genes like PTI5, PR1, HSPs, PALs, CAD, CCoAOMT, and CYPs showed significant differences between L4 and the wild type, suggesting that the expression of these genes is impacted by *MtLOX24* overexpression. CDPKs, CaMCMLs, IFS, JAZ, and other genes were also significantly different between L4 and the wild type upon MeJA treatment, suggesting that they might be important genes involved in JA signaling. This study provides a reference for the study of the response mechanism of *MtLOX24* under MeJA signaling.

Keywords: jasmonic acid; lipoxygenase; transcription; phenylpropanoid; pathogens; hormone

Citation: Xu, L.; Xu, Y.; Lv, H.; Xu, Y.; Wen, J.; Li, M.; Kang, J.; Liu, Z.; Yang, Q.; Long, R. Transcriptomic Analysis Reveals the Mechanism of *MtLOX24* in Response to Methyl Jasmonate Stress in *Medicago truncatula*. *Agriculture* **2024**, *14*, 1076. https://doi.org/10.3390/agriculture14071076

Academic Editor: Antonio Di Matteo

Received: 24 May 2024
Revised: 26 June 2024
Accepted: 28 June 2024
Published: 4 July 2024

1. Introduction

Alfalfa (*Medicago sativa*) is a high-quality and high-yield legume, which is an important cultivated forage crop in northwest China, north China, northeast China, and the Jianghuai

Basin. In recent years, alfalfa has been infected by pests throughout different regions, resulting in reduced yield, quality, and palatability, impacting livestock health [1,2]. Jasmonic acid (JA), MeJA, and jasmonates act as primary immune hormones and signaling molecules for the expression of defense genes in plants, capable of promoting plant defense against mechanical injury, insect attack, and pathogen infection [3]. Exogenous MeJA treatment can simulate experiments related to plant mechanical damage and insect feeding. JA and MeJA have diverse effects on plant growth and development. Exogenous application of high concentrations of MeJA can inhibit the seed germination and root and hypocotyl elongation of plants [4]. This leads to chlorophyll degradation and reduced photosynthesis, elevated plant senescence, and increased lipid peroxidation levels [5]. Application of low concentrations of MeJA can elevate the contents of superoxide dismutase (SOD), catalase (CAT), and peroxidase (POD) and reduce the levels of malondialdehyde (MDA) in plants, which can alleviate the damage produced by abiotic stresses on plants [6]. The application of exogenous JA can promote the accumulation of alkaloids and phytoalexins like isoflavones, mustard oil glycosides, and alfalfa alkaloids [7]. Additionally, the application of exogenous MeJA activates the expression of tannins, flavonoids, anthocyanins, and phytoalexin pathways, as well as associated metabolic genes and transcription factors, with the expression of the LOX gene consistently up-regulated following MeJA treatment [8]. MeJA participates in plant defense through the phenylpropanoid metabolic pathway [9], increases the levels of polyphenol oxidase and protease inhibitors, and induces the production of defense-related proteins, including LOX, polyphenol oxidase (PPO), protease inhibitor (PI), phenylalanine lyase (PAL), and POD [10].

LOX participates in fatty acid synthesis and can also promote oxylipin production, including leaf aldehyde, leaf alcohol, and KODA. Exogenous MeJA, mechanical injury, insect biting, and fungal infection can all activate LOX expression [11–13]. MeJA-responsive LOX genes are primarily expressed in cellular vacuoles and plastids [14]. Overexpression of *TomloxD* in tomato increased the LOX activity and the content of endogenous JA, which participated in endogenous JA synthesis and improved the tolerance to high-temperature stress and pathogen invasion by *Cladosporium fulvum* [15]. In maize, *ZmLOX5* transposon-insertional disruption mutants had limited resistance to insects and were more sensitive to pathogen infestation, with reduced accumulation of linked defense metabolites. The expression of the *ZmLOX5* gene was increased by the exogenous application of 12-OPDA and 9,10-KODA [16,17]. In addition, the lipoxygenase 5-LOX was associated with the generation of ROS in various cells, stimulating cell proliferation and inhibiting apoptosis. Ascorbic acid, quercetin, and polyphenolic compounds can also bind to the 5-LOX active site [18].

Studies have demonstrated that the JA signaling pathway is associated with phenylpropanoids, plant pathogen substances, and terpenoids. Correspondingly, researchers have clarified that JA signaling is composed of protein–protein interaction modules comprising multiple genes, including the JAZ-MYC signaling module [19], the COI1-JAZ coreceptor module, the downstream regulation of JAZ-interacting transcription factors, and multiple negative feedback loops [3]. JA was generated by the oxidation of free linolenic acid by lipoxygenase (13/9-LOX) [20].

The LOX protein participates in the process of JA synthesis and plays an important role in plant development and resistance to stress, but the regulatory mechanism of exogenous MeJA for the LOX gene remains unclear. In this study, *MtLOX24* (MTR_8g018690) was cloned and transformed into *M. truncatula* R108 via *Agrobacterium* infection. Exogenous MeJA treatment and physiological detection of wild-type *M. truncatula*, *MtLOX24* overexpression lines, and the *MtLOX24 Tnt1* mutant were performed. Transcriptomic sequencing was employed to analyze the gene expression profile and functional enrichment in the above genotypes treated with exogenous MeJA and to screen key genes involved in the JA signal transduction of *MtLOX24*.

This study aimed to identify the resistance of *MtLOX24* to exogenous MeJA treatment, and analyze the mechanism of action of *MtLOX24* under MeJA stress to further elucidate the role of the LOXs in regulating the JA signaling pathway.

2. Materials and Methods

2.1. Plant Materials

The *M. truncatula* genotype R108 was utilized as the test material and as a wild-type control for our subsequent experiments. The *M. truncatula* mutant lines were obtained and ordered through the *Medicago truncatula* mutant database (https://medicago-mutant.dasnr.okstate.edu/mutant) (accessed on 24 June 2023). Two mutant lines corresponding to the *MtLOX24* (MTR_8g018690) gene, NF17516 (*lox-1*), and NF16624 (*lox-2*) were identified in the *M. truncatula* mutant database. To identify mutant materials, primers (Supplementary Table S1) were designed based on the genomic sequence, and insertion sites were determined by PCR and PCR-product sequencing. Specifically, two pairs of primers (Supplementary Table S1) were employed for identification, including *MtLOX24* mutant-F and *MtLOX24* mutant-R to detect whether the *MtLOX24* was expressed in the wild-type and mutant materials. The second pair of primers, *MtLOX24* mutant-F and Tnt-R (or LOX mutant-R and Tnt-R), were used to detect whether the mutant contained the Tnt insertion site. The *M. truncatula* seeds were germinated on wet filter paper and transferred to 1/2 Hoagland solution in a growth chamber at conditions of 22/18 °C for a 16/8 h light and dark cycle.

2.2. Cloning of MtLOX24 and Its Genetic Transformation

We previously analyzed the expression patterns of *M. truncatula* and *M. sativa* LOX family genes in response to exogenous MeJA application. From these data, we identified a MeJA-induced lipoxygenase protein (MTR_8g018690), which was named *MtLOX24* [21]. The coding sequence of *MtLOX24* was cloned using primers *MtLOX24*-F and *MtLOX24*-R (Supplementary Table S1). The product was ligated to the expression vector pCAMBIA3301, and the recombinant plasmid *35S::MtLOX24-GUS* was transformed into *Agrobacterium tumefaciens* EHA105 (Huayueyang Biotechnology Co., Ltd., Beijing, China). Genetic transformation of *M. truncatula* R108 was performed using leaf infestation according to the protocol of Chabaud [22]. Two overexpression lines, L4 and L6, were selected for the MeJA treatment experiment, and L4 was selected for subsequent sequencing analysis. Overexpression plants were verified by PCR assay using primers 35S/NC-*MtLOX24*-R (Supplementary Table S1).

2.3. MeJA Treatment of M. truncatula

The seeds of wild-type *M. truncatula* R108, two *MtLOX24*-overexpressing lines (L4 and L6), and two mutants (*lox-1* and *lox-2*) were disinfected and placed in the dark at 4 °C. The cotyledons were fully expanded after germination for 4 to 5 days under a 16/8 h photoperiod at 22/18 °C, and the seedlings were placed into a 1/2 Hoagland nutrient solution. After three weeks of culturing, the seedlings were transferred to a 1/2 Hoagland nutrient solution supplemented with 200 μM of MeJA (Beijing Solarbio Science&Technology Co., Ltd., Beijing, China) for incubation, phenotypes were observed, and plant sampling was performed after seven days.

2.4. Measurement of Physiological Parameters

To detect the physiological changes in *M. truncatula* in the process of the MeJA treatment, the activities of peroxidase (POD), catalase (CAT), and H_2O_2 levels were determined. After the 200 μM MeJA treatment, the leaves of *M. truncatula* were harvested with three biological replicates, each containing 15 seedlings, fully mixed to prevent sample errors in the physiological assays. The physiological parameters were characterized according to the operating methods of the kit, including a peroxidase (POD) activity detection kit, a catalase

(CAT) activity detection kit, and a hydrogen peroxide (H_2O_2) content detection kit from Beijing Solarbio Science&Technology Co., Ltd., Beijing, China.

2.5. Sampling and RNA Extraction

The leaves of *M. truncatula* were snap-frozen in liquid nitrogen and then kept at −80 °C. Each sample contained three replicates, and three biological replicates were established. RNA was extracted using the Promega EastepTM Total RNA Extraction Kit (Promega Biotech Co., Ltd., Beijing, China), followed by cDNA reverse transcription using the Takara PrimeScriptTM Reverse Transcriptase Kit (Takara Biomedical Technology Co., Ltd., Beijing, China).

2.6. Transcriptome Sequencing and De Novo Assembly

Three types of sequencing materials were employed in this experiment, including the wild-type R108, the *MtLOX24*-overexpressing line L4, and the mutant *lox-1*. After total RNA extraction, an Agilent 2100 bioanalyzer (Agilent Technologies Inc., California, USA) was utilized for quality control and RNA integrity detection. The first strand of cDNA was synthesized using oligonucleotide-enriched messenger RNA (mRNA) as a template and random oligonucleotides as a primer. The second strand of cDNA was synthesized using RNaseH, DNA polymerase I, and dNTPs. AMPure XP beads (Beckman Coulter, Brea, CA, USA) were used to screen the cDNA with a length of about 250-300 bp for PCR amplification, and the purified PCR products were obtained to construct a cDNA library. The library was examined using an Agilent 2100 bioanalyzer and sequenced using the Illumina platform (San Diego, CA, USA). The specific process was completed by Novogene Co., Ltd. B. The software Cutadapt 1.9.1 (Dortmund, Germany) was used to remove reads with an adapter, containing N, and low quality. The resulting clean reads were compared and targeted to the reference genome using HISAT2 2.2.1 software (TX, USA) [23]. The reference genome for sequencing and sample participation was the full-length transcriptome (MedtrA17_4.0, accession: GCA_000219495) of *M. truncatula*.

2.7. qRT-PCR Analysis

The gene primers for qRT-PCR in this study were designed using NCBI Primer-BLAST (http://www.ncbi.nlm.nih.gov/tools/primer-blast/, accessed on 10 August 2022), and the primer sequences are shown in Supplementary Table S1. *MtActin* was used as an internal reference for *M. truncatula*. qRT-PCR was conducted with three replicates, and there were three technical replicates for each sample. Expression data were transformed using log2 transform normalization ($2^{-\Delta\Delta Ct}$) [24].

2.8. Differential Expression Gene Screening and Annotation Analysis

De novo assembly of this experimental transcript was performed using the StringTie v2.2.0 software (MD, USA). Before screening differentially expressed genes from each group, subread software was employed to assess and count the number of reads (comparison mass value) covered by each gene (including the newly predicted genes) from start to end. Those with comparison mass values below 10, reads for unpaired comparisons, and reads for comparisons with multiple regions of the genome were screened out [25]. The expression value (FPKM) of all genes in each sample was utilized to measure the expression distribution of unigenes [26].

In this study, the differentially expressed genes were screened using a threshold of padj < 0.05, and the expression difference between the three groups was more than 2-fold. The GO and KEGG pathway of differentially expressed genes enrichment analysis utilized the GO database (http://geneontology.org/, accessed on 20 July 2023), KEGG database (http://www.genome.jp/kegg/, accessed on 20 July 2023), and clusterProfiler 3.10.1 software (Guangzhou, China). The expression patterns of differentially expressed genes were analyzed, and the images were drawn using TBtools-II v2.097 (Guangzhou, China).

2.9. Statistical Analysis

All experiments were conducted in triplicate, and the data were the averages of the three replications. Histograms were drawn using the GraphPad Prism 7.05 software (Chicago, IL, USA). One-way analysis of variance (ANOVA) was performed using SPSS 19.0, and the differences between treatments were evaluated by Duncan analysis at a level of 0.05, with different lowercase letters indicating significant differences ($p < 0.05$).

3. Results

3.1. Identification of Lox Mutants and Generation of MtLOX24 Overexpression Lines

Via PCR detection, two homozygous mutant lines of the *MtLOX24* (MTR_8g018690) gene were identified. The detection of amplification using LOX mutant-F and Tnt1-R primers indicated the forward insertion of *Tnt1* into the *MtLOX24* gene (Figure 1A,B). Through comparison of the sequencing results, the *Tnt1* in NF17516 (*lox-1*) was inserted at 1542 bp downstream of ATG in *MtLOX24*, and NF16624 (*lox-2*) was inserted at 1619 bp downstream of ATG in *MtLOX24*. The insertion sites are illustrated in Figure 1A. In this study, two *MtLOX24* overexpression lines, L4 and L6, obtained via *Agrobacterium*-mediated transformation were selected, and the relative expression levels of *MtLOX24* in the *lox* mutants and overexpression lines were identified by qRT-PCR (Figure 1C).

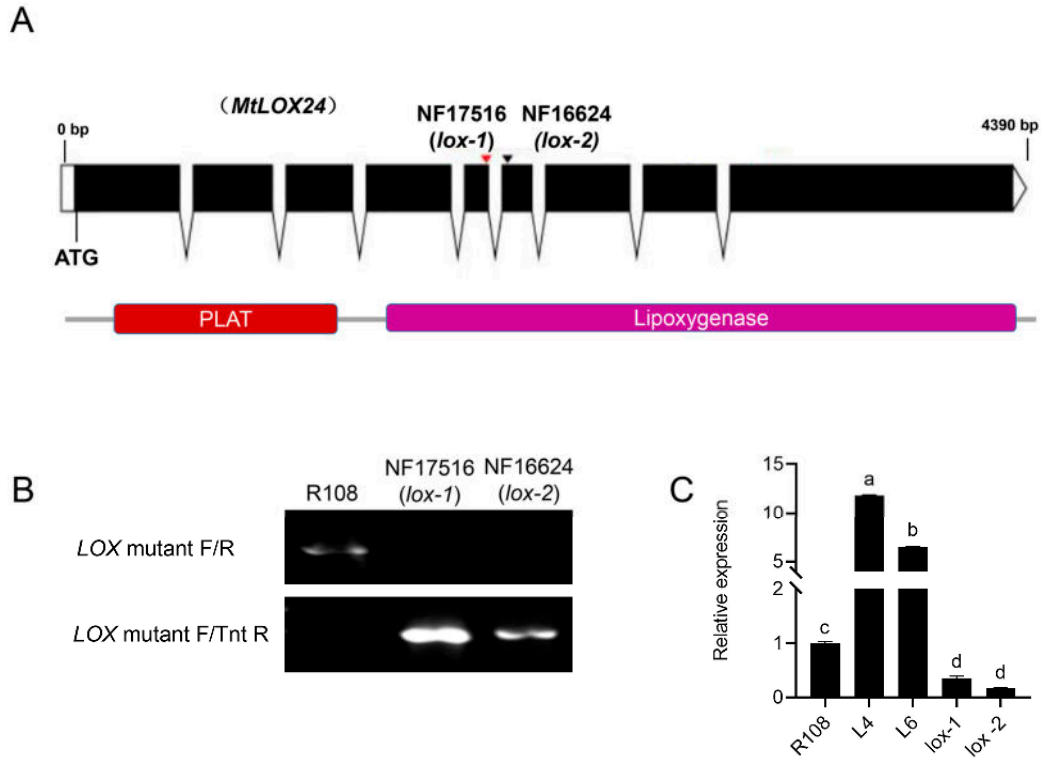

Figure 1. Structure of *MtLOX24* and identification of *lox* mutants in *Medicago truncatula*. (**A**) Structural map of the *MtLOX24* gene (MTR_8g018690). The black boxes represent exons, and the black folded lines are introns. *Tnt1* in the two mutant lines (NF17516, *lox-1*; NF16624, *lox-2*) is located in exon 5 and exon 6 of the *MtLOX24* gene. The *MtLOX24* gene contains two conserved domains, PLAT, and lipoxygenase, which are located between 158-574 bp and 633-2998 bp of the genomic sequence, respectively. (**B**) PCR identification of homozygosity in two *lox* mutant lines. (**C**) qRT-PCR analysis of *MtLOX24* expression levels in overexpression lines and mutants. Different lowercase letters denote significant differences ($p < 0.05$).

3.2. Physiological Characteristics of Medicago truncatula Treated with Exogenous MeJA

To understand the changes in the physiological levels in *M. truncatula* with the 200 μM MeJA treatment, three physiological indicators, catalase (CAT) activity, peroxidase (POD)

activity, and hydrogen peroxide content (H_2O_2), were assessed in wild-type R108, the *MtLOX24* overexpression lines L4 and L6 and the mutants *lox-1* and *lox-2* following MeJA treatment. As shown in Figure 2, the leaves of *M. truncatula* showed wilting and yellowing phenotypes after treatment with 200 μM of MeJA for seven days, in which the mutants *lox-1* and *lox-2* showed more severe symptoms than the overexpression lines L4 and L6 (Figure 2A). By examining the effects of exogenous MeJA on related enzyme activities in *M. truncatula*, we found that the CAT enzyme activities in the overexpression lines L4 and L6 were significantly increased by 2.5-2.8 times relative to the mutants *lox-1* and *lox-2* ($p < 0.05$), but the difference was not significant compared with R108 (Figure 2B). The POD enzyme activity and H_2O_2 levels in the mutants *lox-1* and *lox-2* were significantly higher than those in the overexpression lines L4 and L6 ($p < 0.05$) and were increased by approximately 1.2 and 1.3 times, respectively (Figure 2C,D).

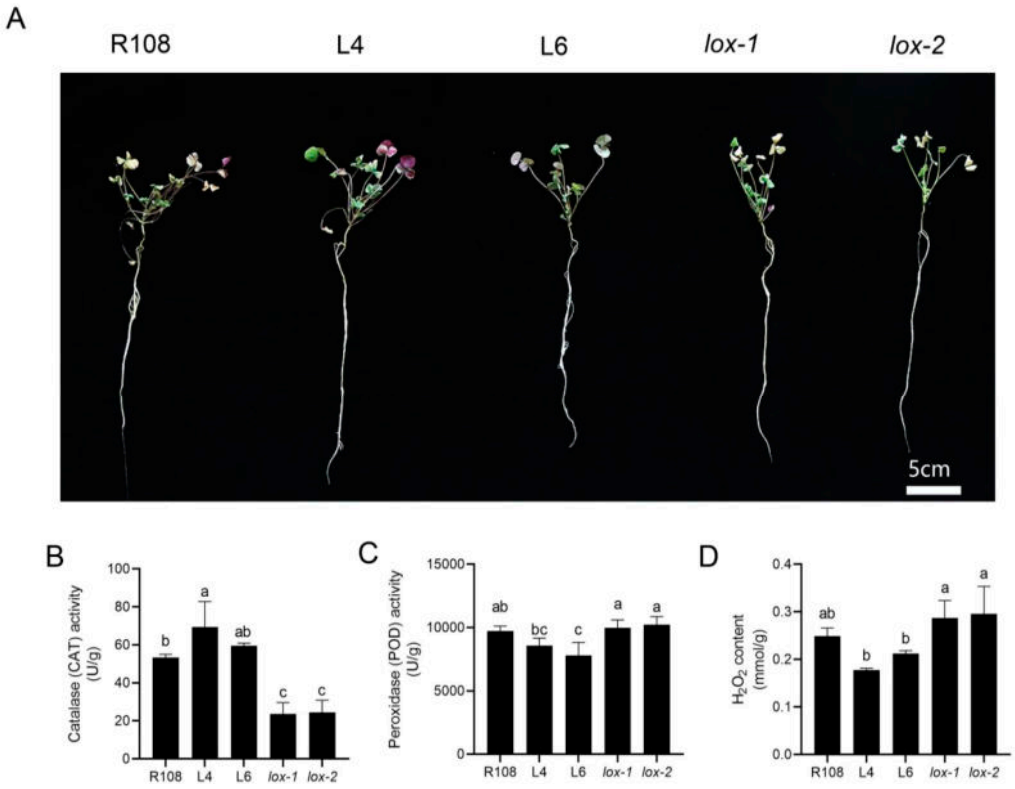

Figure 2. Phenotypic and physiological changes in *Medicago truncatula* treated with MeJA. (**A**) The phenotype of *M. truncatula* growing in 1/2 Hoagland solution treated with 200 μM of MeJA for seven days. (**B**) Detection of the CAT activity in *M. truncatula* treated with 200 μM of MeJA for seven days. (**C**) Detection of POD activity in *M. truncatula* treated with 200 μM of MeJA for seven days. (**D**) Detection of H_2O_2 content in *M. truncatula* treated with 200 μM of MeJA for seven days. Different lowercase letters denote significant differences ($p < 0.05$).

3.3. Sequencing Data Quality Analysis

To examine the possible pathways associated with the *MtLOX24* gene in response to MeJA, RNA was isolated from six samples of *M. truncatula* seedlings under untreated conditions (cR108, cL4, and clox1) and MeJA treatment (R108, L4, and lox1), and cDNA libraries were constructed, with three biological replicates set up for each condition. A total of 18 cDNA libraries were generated, with 783,647,300 original sequence reads obtained. After filtering the raw sequenced data, 117.55 G of original data were obtained. A total of 754,030,364 clean reads for subsequent analysis were obtained by filtering the original data, the sequencing error rate and GC content distribution were examined, and the total number of clean sequences in the 18 cDNA libraries was 113.11 G. The percentage of Q20 bases for each sample was over 98.01, and the percentage of Q30 bases for each sample

was over 94.18, indicating that the quality of the library construction was appropriate (Supplementary Table S2). After filtering out the reads with comparison quality values below 10, the non-comparison of reads in the comparison, and the comparison of reads in multiple regions of the genome, 54,496 unigenes were obtained, of which 3551 were novel genes.

3.4. Expression Patterns and Cluster Analysis of Differentially Expressed Genes (DEGs)

In this study, 18 cDNA libraries were divided into six groups for transcriptomic analysis to analyze the expression of DEGs in the *M. truncatula* wild-type R108, overexpression lines, and mutants with or without MeJA treatment. Three samples were under normal growth conditions (cR108, cL4, and clox1), and three samples were under treatment with MeJA (R108, L4, and lox1). In this study, DESeq2 v1.0 was utilized to screen DEGs, and 10,238 DEGs were identified with the difference between libraries being greater than or equal to two. Among them, we primarily compared the groups under normal growth conditions (cL4 vs. cR108 and clox1 vs. cR108), before and after MeJA treatments (R108 vs. cR108 and L4 vs. cL4), and after MeJA treatment (lox1 vs. R108 and lox1 vs. L4). Under normal growth conditions, cL4 and clox1 contained 557 (483 up-regulated and 74 down-regulated) and 697 (611 up-regulated and 86 down-regulated) DEGs compared with cR108, respectively. Compared with cR108 and cL4 before treatment, MeJA-treated R108 and L4 contained 7801 (4770 up-regulated and 3031 down-regulated) and 6184 (3523 up-regulated and 2661 down-regulated) DEGs, respectively. Following MeJA treatment, lox1 had 626 (326 up-regulated and 300 down-regulated) DEGs compared with R108, and 1010 (539 up-regulated and 471 down-regulated) DEGs compared with L4 (Figure 3A).

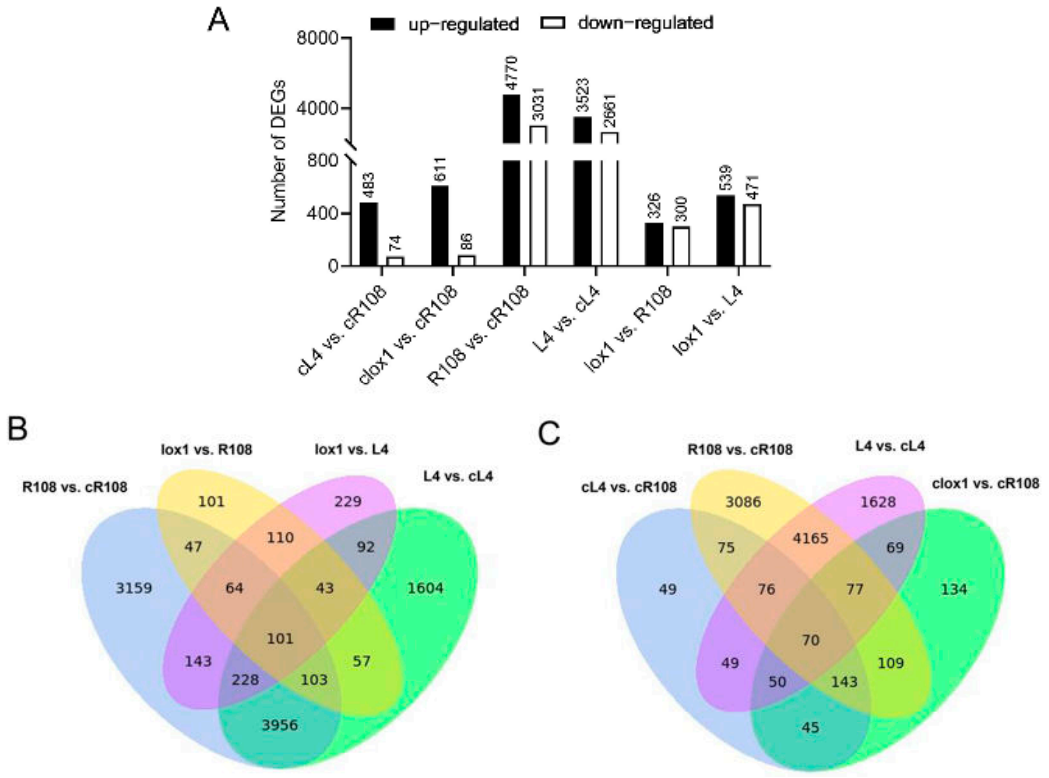

Figure 3. Statistical analysis of DEGs. (**A**) Summary of the DEGs across different comparison groups. (**B**,**C**) Venn diagrams depicting different comparison combinations represent the number of relevant DEGs that MeJA processed and the overlap of sets obtained in each comparison.

By analyzing the overlapped DEGs among the four comparisons (R108 vs. cR108, L4 vs. cL4, lox1 vs. R108, and lox1 vs. L4) using venn diagrams (Figure 3B), we found 4,388 genes with common changes between R108 and L4 with or without MeJA treatment,

accounting for the largest proportion of DEGs. Following MeJA treatment, there were 318 common genes in lox1 vs. R108 and lox1 vs. L4 between the two comparison groups, and 101 common DEGs between the four comparison groups. By examining the overlapped DEGs among the four comparisons of cL4 vs. cR108, clox1 vs. cR108, R108 vs. cR108, and L4 vs. cL4 (Figure 3C), under normal growth conditions, cL4 vs. cR108 and clox1 vs. cR108 had 308 common genes and 70 DEGs between the four comparison combinations.

The expression patterns of all DEGs were investigated ($p < 0.05$) and divided into 20 expression patterns (Figure 4A), encompassing several groups of opposite expression patterns. Specifically, the levels of L4 and cL4 expression in profile 2 and profile 17 were the lowest and highest, and the expression patterns were opposite. lox1 and clox1 in profile 3 and profile 16 were different from the other two materials and had opposite expression patterns. In addition, the cluster analysis of all DEGs is shown in Figure 4B.

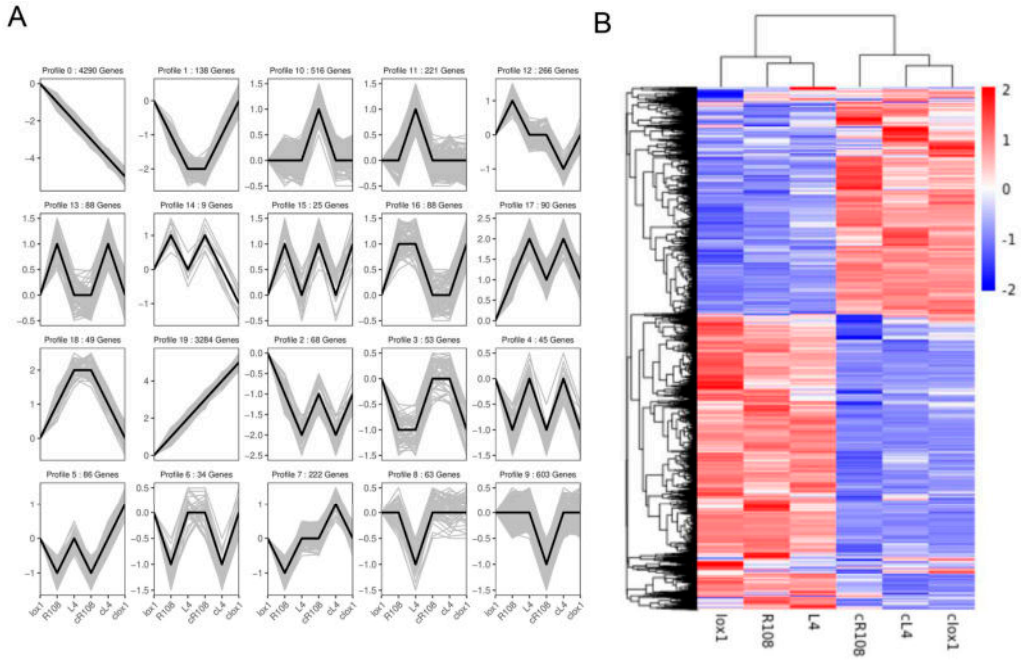

Figure 4. Expression pattern analysis of DEGs. (**A**) Analysis of expression patterns of DEGs. (**B**) Heatmap of expression patterns of DEGs. Heatmaps were performed with the normalization method standard score on log2-transformed data. Red and blue indicate up- and down-regulation.

3.5. GO Enrichment Analysis of DEGs

Through GO annotation analysis of all unigenes, 50 GO categories were obtained. These GO categories mainly included biological processes, cellular components, and molecular functions. Among them, biological processes had the greatest number of unigenes, followed by cellular components and molecular functions. In the category of biological processes, the highest percentage were cellular processes (19,315, 21.7%), metabolic processes (17,227, 19.4%), and single-organism processes (12,489, 14.05%). In the category of cellular components, the highest proportions were cell (15,668, 20.55%), cell part (15,668, 20.55%), membrane (11,782, 15.45%), and organelle (11,169, 14.65%). Among the molecular functions, the highest percentages were binding (19,041, 47.82%), catalytic activity (15,271, 38.35%), and transporter activity (1819, 4.57%) (Supplementary Figure S1).

After obtaining the DEGs through gene expression analysis, functional annotation was performed on all the DEGs to understand their functions. In this study, the clusterProfiler was employed for the GO functional enrichment analysis of the DEGs, and a padj value of less than 0.05 was used as the threshold of significant enrichment. The results revealed that a total of 122 significantly enriched GO categories were in the R108 vs. cR108 group, with the most enriched categories in the biological process category (79, 64.75%). There were 112 significantly enriched GO categories in the L4 vs. cL4 group, with the most enriched

in the biological process category (57, 50.89%). Additionally, there were 40 significantly enriched GO categories in the clox1 vs. cR108 group, among which there were 28 categories of biological processes. A total of 65 significantly enriched GO categories were identified in cL4 vs. cR108, with 64 categories being the most enriched in the biological processes.

By comparing normal growth conditions and MeJA-treated R108 (R108 vs. cR108 group), they were mainly enriched in the biological processes of glutathione metabolism, acid chemicals, toxic substances, and drug response. Molecular functions were mainly enriched in glutathione transferase activity, UDP-glycosyltransferase activity, UDP-glucosyltransferase activity, and chitinase activity. The cellular components mainly encompassed the respiratory chain and related complexes. The comparison between L4 under normal growth conditions and L4 with MeJA treatment (L4 vs. cL4) revealed that the most significantly enriched biological processes and molecular functions were essentially consistent with those of the R108 vs. cR108 group comparison, but there were differences in cellular components, with enrichment in the chloroplast membrane, chloroplast stroma, and plastid membrane. By comparing the DEGs in the overexpression lines, the *lox* mutants, and R108 under normal conditions (clox1 vs. cR108 and cL4 vs. cR108 groups), it was identified that their DEGs were enriched in the biological processes of synthesis and metabolism of benzene compounds and salicylic acid metabolism. Molecular functions associated with calcium-ion binding were also enriched. When the significantly enriched groups were greater than 15, only 15 categories were selected for illustration (Figure 5; Supplementary Table S3).

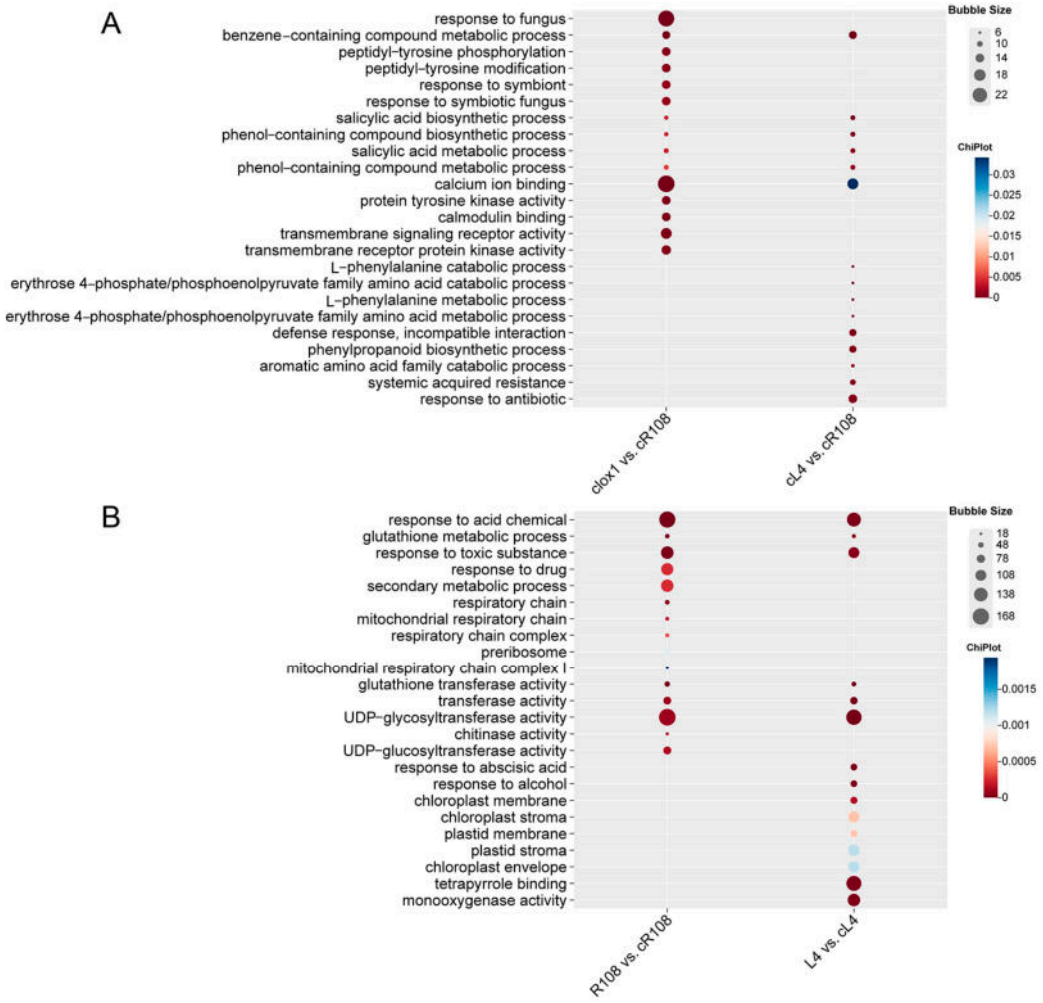

Figure 5. GO classification of DEGs. (**A**,**B**) GO enrichment analysis of clox1 vs. cR108, cL4 vs. cR108, R108 vs. cR108, and L4 vs. cL4 DEGs. The size of each dot represents the number of genes annotated with the GO term, and the color from red to blue represents the significance of the enrichment.

3.6. KEGG Enrichment Analysis of DEGs

KEGG (Kyoto Encyclopedia of Genes and Genomes) is a comprehensive database integrating genomic, chemical, and system function information. In this study, clusterProfiler was employed for the KEGG enrichment analysis of all DEGs, and a padj value of less than 0.05 was used as the threshold for significant enrichment. If there were over ten significant enrichment pathways, the first ten enrichment pathways were mapped and analyzed.

The DEGs of R108 (R108 vs. cR108 group) under normal growth conditions and MeJA treatment were mainly enriched across 124 KEGG pathways, and 11 pathways were significantly enriched. These pathways included glutathione metabolism, phenylpropanoid biosynthesis, the MAPK signaling pathway, circadian rhythm, α-linolenic acid metabolism, flavonoid biosynthesis, amino sugar and nucleotide sugar metabolism, galactose metabolism, plant–pathogen interactions, tropane, piperidine and pyridine alkaloid biosynthesis, and proteasome (Figure 6A). The comparison of L4 with or without MeJA under normal growth conditions (L4 vs. cL4) revealed that DEGs were mainly enriched in 123 KEGG pathways, and 7 pathways were significantly enriched, which was similar to the significantly enriched pathways in the R108 vs. cR108 comparison. In addition, this group was also enriched in the biosynthesis of various plant secondary metabolites and photosynthetic antenna proteins (Figure 6B).

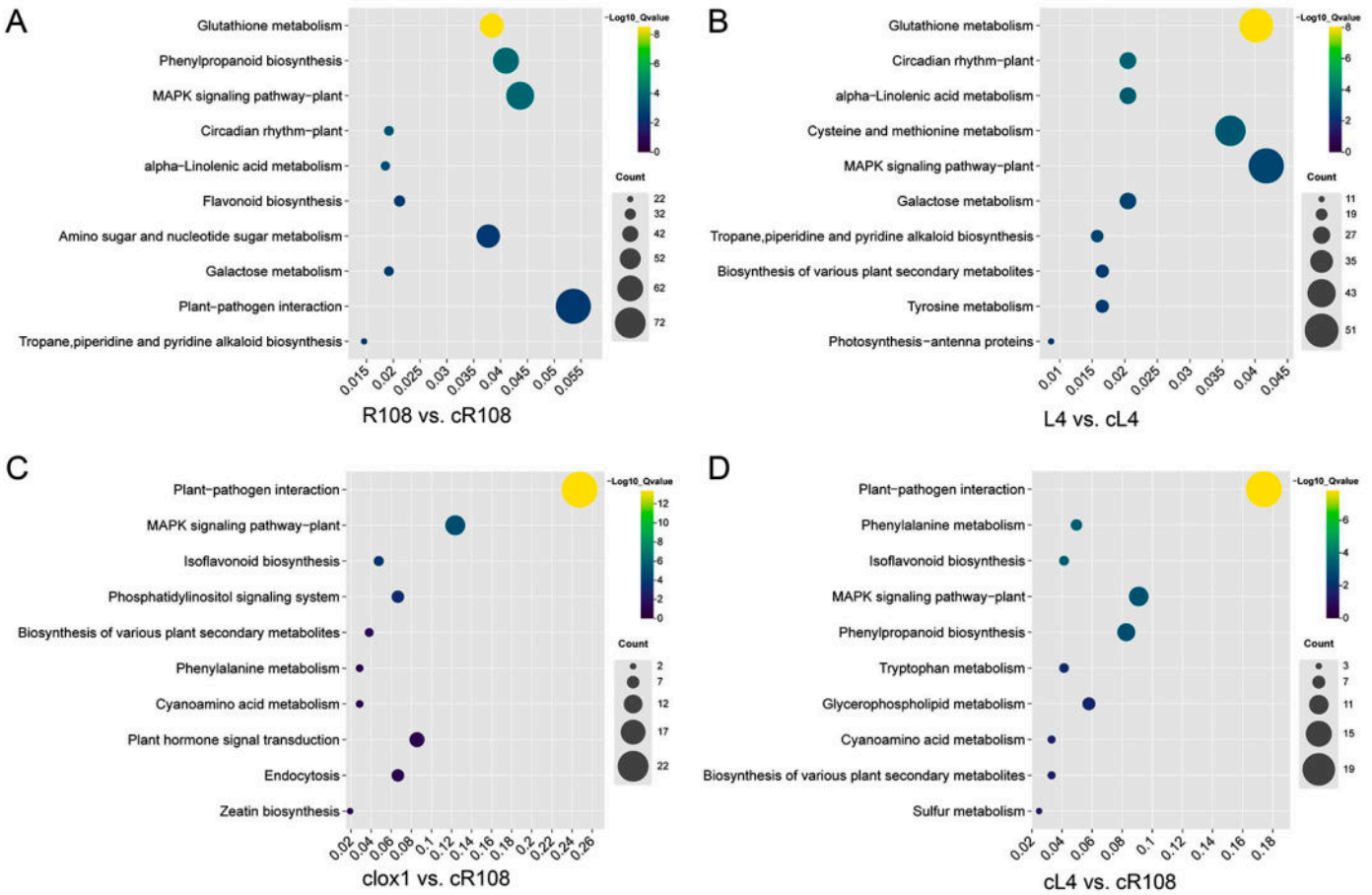

Figure 6. KEGG pathway enrichment scatter diagrams of DEGs. (**A**–**D**) KEGG enrichment analysis of R108 vs. cR108, L4 vs. cL4, clox1 vs. cR108, and cL4 vs. cR108 DEGs. The size of each dot represents the number of genes annotated with the KEGG term, and the color from blue to yellow represents the significance of the enrichment.

By comparing the DEGs in the clox1 vs. cR108 group under normal growth conditions, 58 KEGG pathways were predominantly enriched, and 4 pathways were significantly enriched. These pathways included plant–pathogen interactions, the MAPK signaling pathway, isoflavonoid biosynthesis, the phosphatidylinositol signaling system, the biosynthesis of various plant secondary metabolites, phenylpropanoid biosynthesis, cyanoamino acid metabolism, plant hormone signal transduction, endocytosis, and zeatin biosynthesis (Figure 6C). In the untreated cL4 vs. cR108 group, DEGs were mainly enriched in 77 KEGG pathways, and 5 pathways were significantly enriched. These included plant–pathogen interactions, phenylalanine metabolism, isoflavonoid biosynthesis, the MAPK signaling pathway, phenylpropanoid biosynthesis, tryptophan metabolism, glycerophospholipid metabolism, cyanoamino acid metabolism, the biosynthesis of various plant secondary metabolites, and sulfur metabolism (Figure 6D).

3.7. Analysis of DEGs and Related Pathways in Response to MeJA Stress in M. truncatula

Through transcriptome analysis, the DEGs were identified to be significantly enriched in pathways like phenylpropanoid biosynthesis, plant–pathogen interactions, and plant hormone signal transduction. Key DEGs between the treatment groups were identified by comparing the expression patterns of genes in R108, L4, and lox1 with or without MeJA treatment in significantly enriched pathways. Under MeJA treatment conditions, overexpression of *MtLOX24* would likely cause changes in the transcription levels of genes in related pathways.

3.7.1. Analysis of DEGs Related to Plant–Pathogen Interactions

The plant–pathogen interaction pathway encompassed multiple mechanisms, including pathogen recognition, signal transduction, and the activation and expression of resistance genes [27]. In this study, we found that DEGs in the plant–pathogen interaction pathway were enriched in the cL4 vs. cR108, clox1 vs. cR108, R108 vs. cR108, lox1 vs. R108, and lox1 vs. L4 groups, and metabolic pathways associated with plant–pathogen interactions were mapped according to the mtr04626 pathway (https://www.kegg.jp/pathway/mtr04626) (accessed on 24 June 2023). Among them, four resistance genes, including PTI5 (MTR_2g015040), PRB1 (MTR_2g012370), PR1C (MTR_2g010600), and PIK2 (MTR_5g027860), were up-regulated in the cL4 vs. cR108 group, and FPKM was increased by 1.6 to 33.5 times. The heat shock protein (MTR_1g025430, MTR_5g096460, and MTR_5g096430) was up-regulated in the cL4 vs. cR108 group, with FPKM increased by 1.2 to 2.4 times. Fifteen genes were significantly regulated by Ca^{2+} signaling, which were up-regulated in the lox1 vs. R108 and lox1 vs. L4 groups, including one RBOHB gene (MTR_7g113130), ten CaMCMLs (MTR_3g067610, MTR_4g103650, MTR_5g079340, MTR_7g090450, MTR_2g098890, MTR_6g025320, MTR_4g103630, MTR_5g017550, MTR_7g074240, and MTR_4g122260), and four CDPKs (MTR_7g106710, MTR_4g066660, MTR_5g022030, and MTR_7g091890). Meanwhile, MPK3 (MTR_4g061130) and MMK2 (MTR_8g028720), related to the MAPK (mitogen-activated protein kinase) pathway, as well as the KCS gene (MTR_2g054940), related to fatty acids carbon chain association, were up-regulated in the lox1 vs. R108 and lox1 vs. L4 groups (Figures 7 and 8).

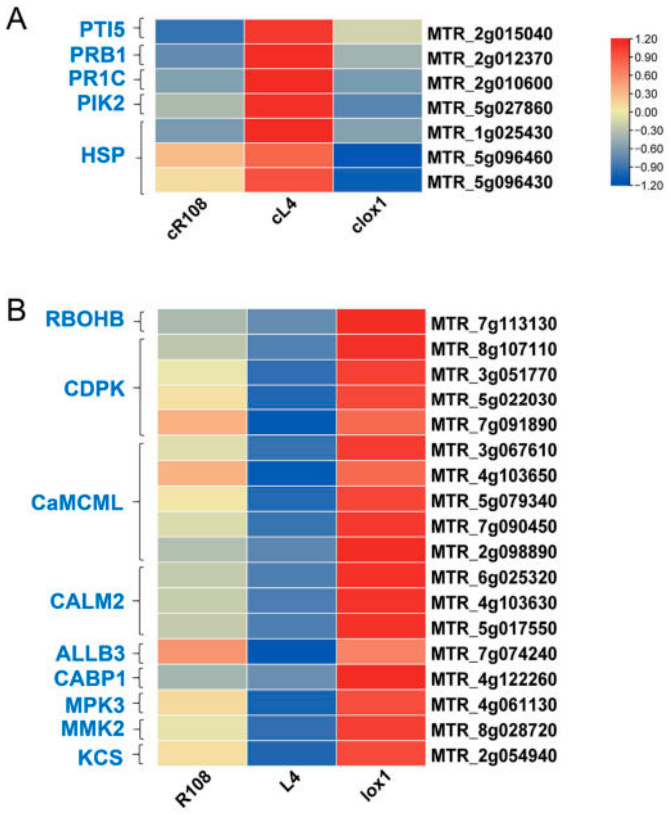

Figure 7. Heatmaps of the expression levels of plant–pathogen interaction-related DEGs. (**A**) Heatmap of DEGs associated with plant–pathogen interactions without MeJA treatment. (**B**) Heatmap of DEGs associated with plant–pathogen interactions with MeJA treatment. Heatmaps were generated with the normalization method standard score using log2-transformed data. Red and blue indicate up- and down-regulation.

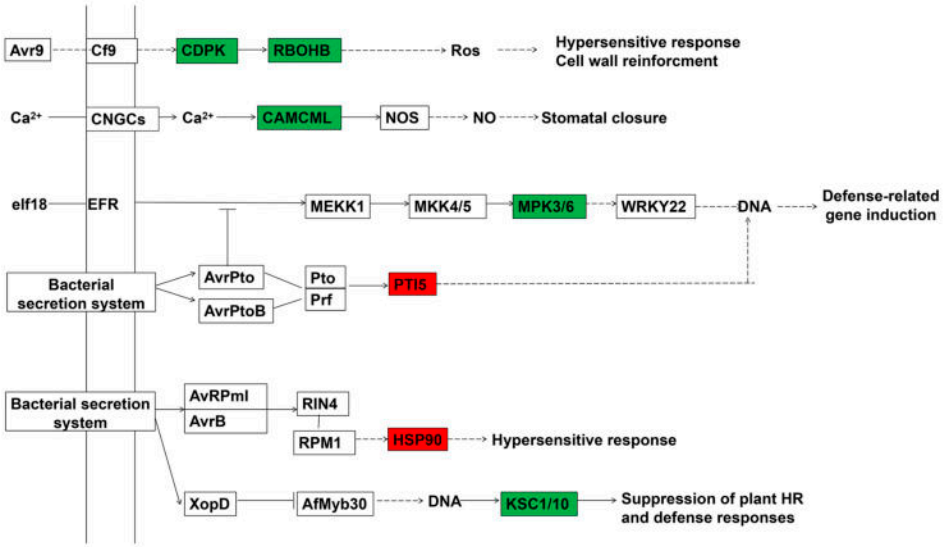

Figure 8. Metabolic pathways and DEGs associated with plant–pathogen interactions. Red boxes show the overexpression line L4 has an increased expression level compared with the wild-type R108. Green boxes show the overexpression line L4 has a lower expression level compared with the wild-type R108.

3.7.2. Analysis of DEGs Related to Phenylpropanoid Biosynthesis

The biosynthesis of phenylpropanoids is an essential means of synthesizing secondary metabolites in plants and is important for plant defense. The synthesized products in-

cluded simple phenylpropanoids, flavonoids, and lignans. KEGG enrichment analysis in R108 vs. cR108, clox1 vs. cR108, cL4 vs. cR108, lox1 vs. R108, and lox1 vs. L4 demonstrated that the phenylpropanoid biosynthesis, isoflavonoid biosynthesis, and phenylalanine metabolism related to phenylpropanoids were significantly enriched, and metabolic pathways associated with plant phenylpropanoid were mapped according to mtr00940 (https://www.kegg.jp/entry/mtr00940) (accessed on 24 June 2023). Fifteen genes associated with phenylpropane synthesis, including two PAL genes (MTR_1g064090 and MTR_5g098720), three CAD genes (MTR_1g025950, MTR_1g107425, and MTR_6g086340), one FOMT gene (MTR_4g094368), one 4CL1 gene (MTR_4g005750), and two CCoAOMT genes (MTR_4g085590 and MTR_4g094815) were up-regulated in the cL4 vs. cR108 group. Four PRX genes (MTR_2g084010, MTR_2g084020, MTR_3g094630, and MTR_3g466200) and two CSE genes (MTR_4g127220 and MTR_1g115535) were up-regulated in the lox1 vs. R108 and lox1 vs. L4 groups. Isoflavones were mainly produced by cytochrome P450 enzymes of the CYP93C subfamily. In this pathway, CYP81E1/E7 (MTR_4g094775) and two CYP93C genes (MTR_1g105020 and MTR_4g088195) were up-regulated in the cL4 vs. cR108 group. Two IFS genes (MTR_1g105020 and MTR_5g005850) were up-regulated in the lox1 vs. R108 and lox1 vs. L4 groups. In addition, the CAO gene (MTR_1g104590) and TYDC2 gene (MTR_7g098700), which are involved in phenylalanine metabolism, were also up-regulated in lox1 vs. R108 and lox1 vs. L4 (Figures 9 and 10).

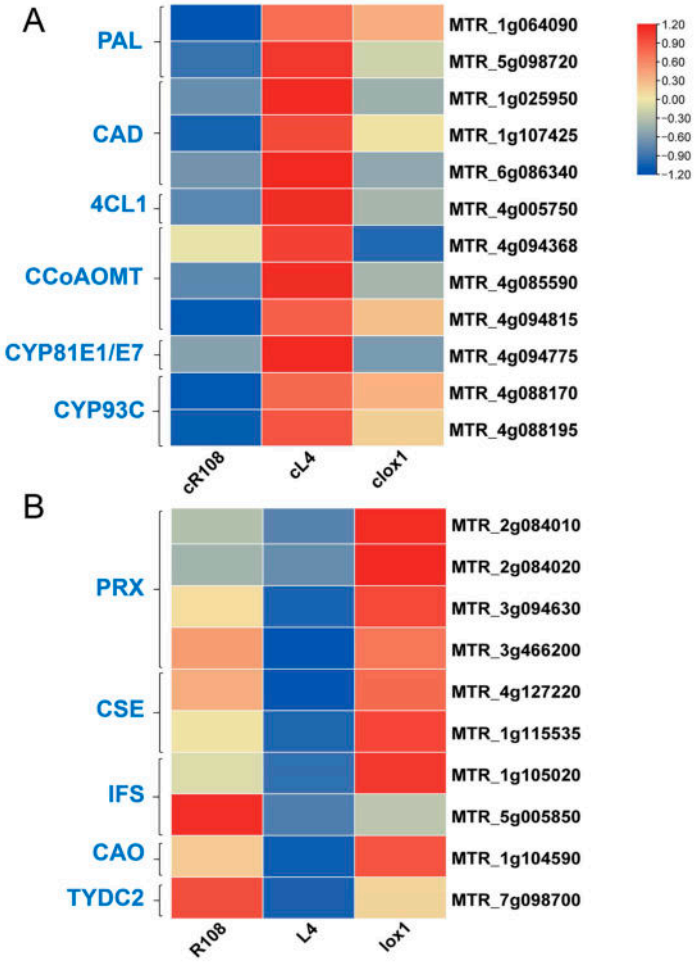

Figure 9. Heatmaps of the expression levels of phenylpropanoid biosynthesis-related DEGs. (**A**) Heatmap of DEGs associated with phenylpropanoid biosynthesis without MeJA treatment. (**B**) Heatmap of DEGs associated with phenylpropanoid biosynthesis with MeJA treatment. Heatmaps were generated with the normalization method standard score using log2-transformed data. Red and blue indicate up- and down-regulation.

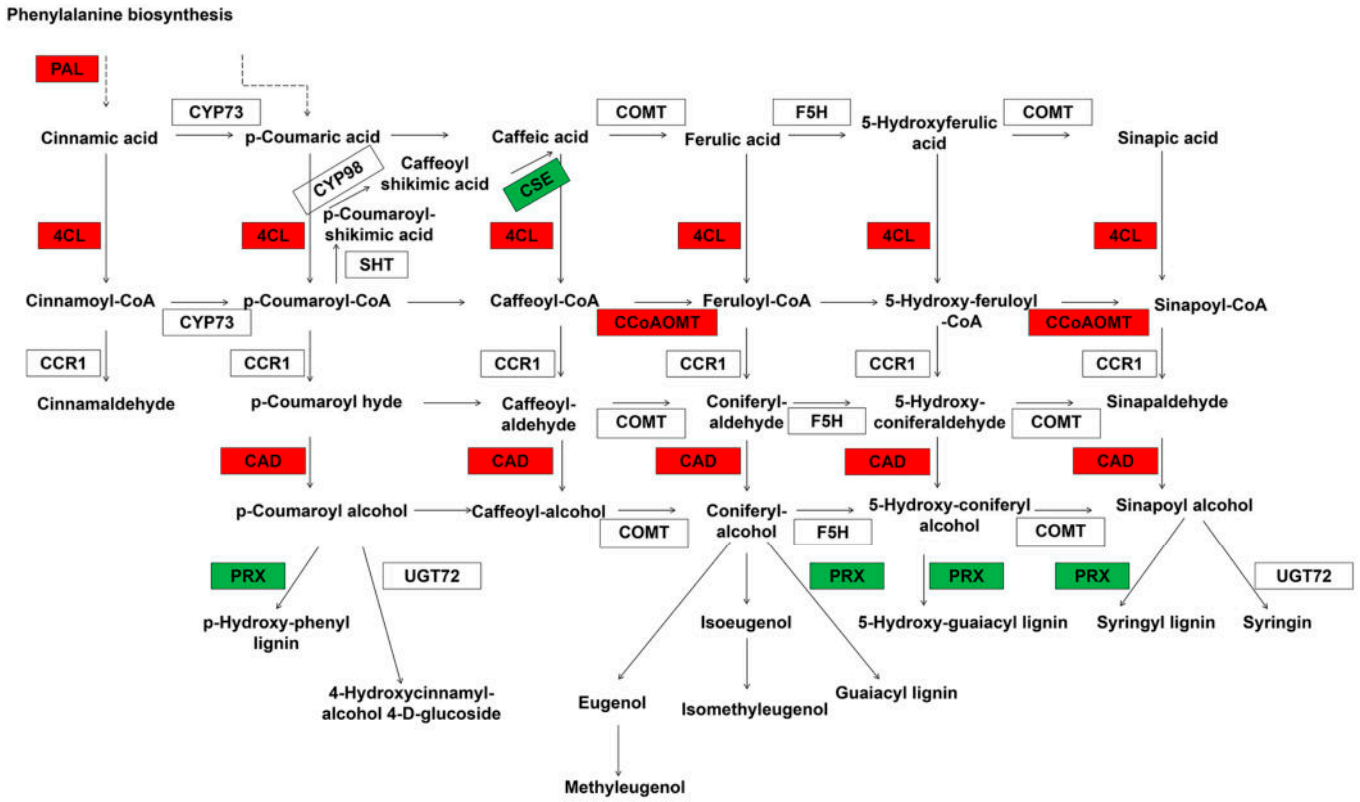

Figure 10. Metabolic pathways and DEGs associated with plant phenylpropanoids. Red boxes show the overexpression line L4 has an increased expression level compared with the wild-type R108. Green boxes show the overexpression line L4 has a lower expression level compared with the wild-type R108.

3.7.3. Analysis of DEGs Related to Plant Hormones

Hormones play important roles in plant resistance signaling pathways. In this study, KEGG enrichment analysis demonstrated that the plant hormone signal transduction metabolic pathway was significantly enriched in all DEGs, and metabolic pathways associated with plant hormones were mapped according to mtr04075 (https://www.kegg.jp/entry/mtr04075) (accessed on 24 June 2023). The JA signal regulates plant morphology and responses to abiotic and biotic stresses. The JAZ gene (MTR_5g013530, MTR_8g021380, and MTR_2g042900) of the jasmonic acid ZIM-domain protein was up-regulated in the lox1 vs. R108 and lox1 vs. L4 groups. PYL4 (MTR_7g070050) is a gene related to carotenoid biosynthesis, which was down-regulated in the lox1 vs. L4 group. In contrast, PP2C (MTR_1g028300) expression was up-regulated in lox1 compared with L4 (Figure 11). This opposite pattern of expression of PYL4 compared with PP2C is consistent with PYL4 inhibiting PP2C (Figure 12). EBF1/2 (MTR_1g012520) is involved in the cysteine and metal metabolism process and was up-regulated in lox1 vs. R108 and lox1 vs. L4. The AAUX/IAA gene (MTR_1g040675, MTR_4g115075, and MTR_1g070520), which plays an important role in cell enlargement and plant growth, was down-regulated in the lox1 vs. L4 group. Moreover, PR genes (MTR_2g010600, MTR_2g010590, and MTR_2g012370), which are involved in plant disease resistance and associated with salicylic acid, were up-regulated in the cL4 vs. cR108 group, suggesting that overexpression of the *MtLOX24* gene induces the expression of PR genes (Figures 11 and 12).

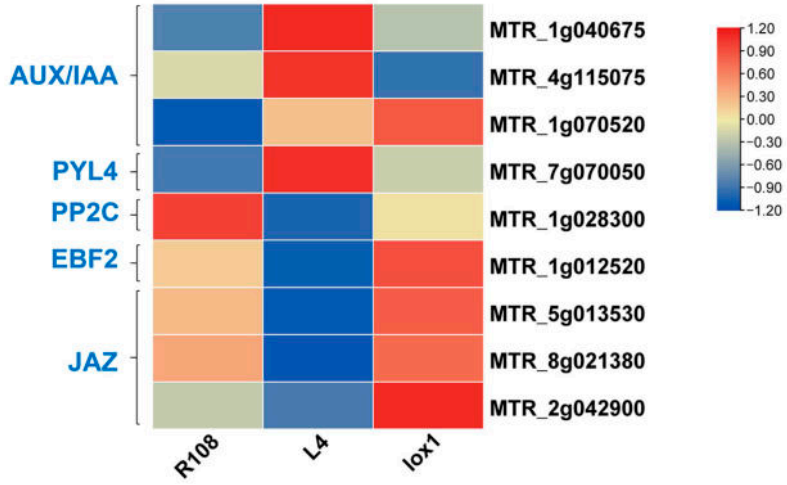

Figure 11. Heatmap of the expression levels of plant hormone-related DEGs with MeJA treatment. Heatmap was generated with the normalization method standard score using log2-transformed data. Red and blue indicate up- and down-regulation.

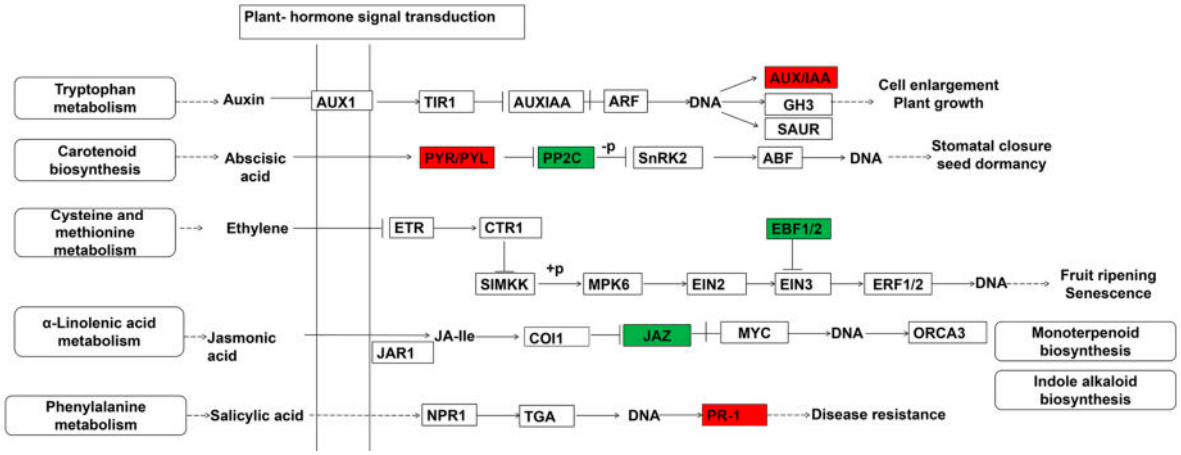

Figure 12. Metabolic pathways and DEGs associated with plant hormone signal transduction. Red boxes show the overexpression line L4 has an increased expression level compared with the wild-type R108. Green boxes show the overexpression line L4 has a lower expression level compared with the wild-type R108.

4. Discussion

MeJA is a common secondary compound and can act as a signaling molecule in response to biotic and abiotic stresses in plants [28]. Studies have shown that MeJA affects the activities of antioxidant enzymes (CAT, SOD, and APX) and the levels of glutathione, chlorophyll b, and carotenoid. MeJA can also alter the activities of arginine decarboxylase (ADC), extracellular invertase, and Rubisco-activating enzyme [29]. In this study, overexpression of *MtLOX24* significantly elevated the activity of CAT under MeJA treatment (Figure 2B) as a defense against the damage produced by high concentrations of MeJA in *M. truncatula*. Our results are consistent with findings in *Glycyrrhiza uralensis*, kiwifruit, and peach [30–32]. In contrast, overexpression of *MtLOX24* significantly reduced the activity of POD under MeJA treatment compared with the control. The activities of POD and H_2O_2 in the mutants *lox-1* and *lox-2* were significantly elevated after MeJA treatment, which may be attributed to the ability of MeJA to induce the effective accumulation of reactive oxygen species (H_2O_2 and O^{2-}) in the plant, resulting in the yellowing and wilting of the leaves in the mutants *lox-1* and *lox-2* after MeJA treatment (Figure 2A).

According to previous research, 30 LOX family genes in *M. truncatula* were identified and classified into 9-LOX and 13-LOX subfamilies. Among them, 13-LOXs were induced

by MeJA and predicted to function in the JA signaling pathway [21]. In this study, by transcriptome analysis of the expression patterns of the DEGs in the cR108 vs. R108 group, we found that most of the *M. truncatula* LOX family genes were significantly induced by MeJA, except for the 9-LOX family members *MtLOX1*, *MtLOX2,* and *MtLOX8*. After MeJA treatment, transcriptional level analysis was performed on the expression of LOX genes in the lox1 vs. R108 and lox1 vs. L4 groups. We found that MeJA treatment significantly induced the expression of *MtLOX24* in the overexpression line L4 and the wild-type R108, with the highest expression found in the overexpression line L4 (Supplementary Figure S2). This finding aligned with the phenotype in Figure 2, indicating that *MtLOX24* positively regulated the resistance of *M. truncatula* to MeJA. Moreover, some genes had opposite expression patterns to *MtLOX24,* including *MtLOX7* and *MtLOX19* in the mutant *lox-1* after MeJA treatment, which were up-regulated compared with the wild-type and overexpression lines.

Transcriptome analysis demonstrated that under normal growth conditions, overexpression or disruption of the *MtLOX24* gene resulted in the significant enrichment of phenylpropanoid metabolism and pathogen-related DEGs. Under MeJA treatment, the overexpression or disruption of the *MtLOX24* gene caused changes in the transcriptional levels of a large number of genes, mainly enriched in phenylpropanoid, pathogen-related, and hormone-related pathways. The key genes affected by *MtLOX24* were also different when MeJA was or was not added. MeJA has been reported to increase the activity of enzymes involved in phenylpropanoid synthesis (PAL, C4H, and 4CL, among others), catalyzing a series of reactions to produce secondary metabolites such as simple phenylpropanoid analogs, phenolics, flavonoids, and lignans, which are required for the wound-healing process [9]. Flavonoids and anthocyanins operate as antiviral agents and antioxidants to directly protect plants from biotic and abiotic stresses. O-methyltransferase (OMT) has two subfamilies, the caffeoyl coenzyme A OMT (CCoAOMT) subfamily and the caffeic acid OMT (COMT) subfamily, in which CCoAOMT is involved in lignin synthesis and regulates the synthesis process of flavonoids and anthocyanin-like substance compounds [33]. The cinnamyl alcohol dehydrogenase (CAD) gene can synthesize p-coumaroyl alcohol, caffeoyl alcohol, coniferyl alcohol, 5-hydroxy-coniferyl alcohol, and sinapoyl alcohol. CAD is involved in lignin synthesis and the development of plant stems [34]. Additionally, peroxidase (PRX) is involved in lignin synthesis and phytolignification in *A. thaliana* and maize [35]. To better understand the relationship between phenylpropanoid genes and metabolites, differentially expressed genes and differentially accumulated metabolites were mapped onto KEGG pathway maps (Figure 10). We found that PAL, 4CL, CCoAOMT, and CAD, which are involved in phenylpropanoid synthesis, were induced in the overexpression line compared with the control under normal growth conditions, while CYP93C and CYP81E were also up-regulated and expressed in the overexpression line. When fungi or bacteria infect plant organs, or when plant microorganisms and insects feed on plants, they activate the activities of natural products such as isoflavones and triterpenes and accumulated triterpene saponins after trauma reaction and MeJA treatment [36]. Following MeJA treatment, the expression of the isoflavone synthesis skeleton (IFS) was significantly reduced in the *MtLOX24*-overexpressing line compared with the control R108, and the expression of the phenylpropanoids synthesis genes (PRX and CSE) and phenylpropanoid metabolism genes (CAO and TYDC2) also demonstrated the same expression pattern. It is speculated that *MtLOX24* might negatively regulate the expression of these genes under the action of MeJA.

Plants have evolved adaptive immune mechanisms in response to invading pathogens. These responses include the pamp-triggered immune response (PTI) to pathogen perception by cell surface pattern recognition receptors (PRRs), the MAPK signaling pathway triggered by FLS2 and EFR activation, and reactive oxygen species and stomatal regulatory responses induced by changes in the concentration of Ca^{2+}. The MeJA-mediated signaling process involves Ca^{2+}, which affects the antioxidant capacity of plants and phenolic compound accumulation [37]. Moreover, Ca^{2+}-binding proteins (CBL, CPK, CaM, and CaMCML) are

known as Ca^{2+} sensors, acting as signaling agents in plant immunity [38]. HSP90 and Ca^{2+}-dependent nucleases play a role in plant hypersensitive cell death, which has been reported in rice [39]. In this study, DEGs and metabolites associated with plant–pathogen interactions were mapped onto the KEGG pathways (Figure 8). The expressions of the pathogen-associated genes PTI5, PR1, and PIK2 were up-regulated. The HSP90 gene involved in the process of hypersensitivity (HR) was also induced in the overexpressing line L4 compared with the control under normal growth conditions, and similar results were found in tomato. Overexpression of the 13-lipoxygenase *TomloxD* promoted the expression of the tomato defense genes *LeHSP90*, *LePR1*, *LePR6*, and *LeZAT* [15], suggesting that *MtLOX24* may also play a role in plant defense. The expression of CaMCMLs and CDPKs was suppressed in the overexpression line L4 following MeJA treatment compared with the control. The expression of the MAP kinase genes MPK3 (MTR_4g061130) and MMK2 (MTR_8g028720), which are involved in plant immune processes, as well as the expression of the β-ketoacyl-CoA synthetase (KCS) gene, which is linked to very-long-chain monounsaturated fatty acid (VLCFA) synthesis, was also inhibited [40]. In contrast, in the mutant *lox-1*, these genes were up-regulated. It is speculated that *MtLOX24* may negatively regulate the expressions of CaMCMLs, CDPKs, MPK3, MMK2, and KCS under MeJA treatment conditions.

JA and salicylic acid (SA) are two major defense hormones, and the synergistic or antagonistic relationship between them is related to the types of hosts and pathogens [41]. JAZ proteins are key transcriptional suppressors during JA signaling. When a plant is not infected by a pathogen, the JAZ protein interacts with ET transcription factors to inhibit the transcriptional activity in the absence of JA. When plants are infected by pathogens in the presence of JA, it is found that EIN3 and EIL1 are released, and transcription is immediately initiated [42]. Additionally, EBF1/2 negatively regulates the ethylene response by degrading EIN3 via ubiquitination or other approaches [43]. In this study, the expression level of the JAZ gene in the *MtLOX24* overexpression line was lower than that in R108 under MeJA treatment, whereas JAZ was significantly induced in the mutant *lox-1*, suggesting that *MtLOX24* negatively regulates the expression of JAZ. EBF1/2, which is involved in fruit ripening and plant senescence in the ethylene response [44], was down-regulated in the overexpression lines treated with MeJA. The ABA signaling pathway plays an important role in abiotic stresses such as salt and drought. ABA binds to the PYR/PYL complex to inhibit PP2C expression, while SnRK2 activates and promotes the expression of downstream transcription factors [45]. In this study, MeJA treatment promoted the expression of PYL in the overexpression line while inhibiting the expression of PP2C. We speculated that *MtLOX24* might be involved in the ABA signaling pathway under MeJA induction. Auxin regulates cell enlargement and plant growth by promoting the expression of Aux/IAA proteins. Compared with wild-type R108, Aux/IAA was up-regulated in the overexpression line after MeJA treatment, indicating that Aux/IAA expression is positively regulated by *MtLOX24* under MeJA treatment.

5. Conclusions

Under exogenous MeJA treatment, overexpression of *MtLOX24* can increase the resistance of *M. truncatula* of MeJA and limit oxidative damage. In this study, libraries were constructed for *M. truncatula* wild-type R108, the *MtLOX24* overexpression line L4, and the *MtLOX24* mutant *lox-1* of *M. truncatula* under normal conditions and MeJA treatment using transcriptome sequencing technology, and the differentially expressed genes among the three materials were obtained. Through GO and KEGG enrichment analysis, important regulatory pathways were found to be associated with *MtLOX24* involved in the MeJA response, including plant–pathogen interactions, phenylpropanoid biosynthesis, and plant hormone signal transduction pathways, and related genes were excavated. Under normal growth conditions, PTI5, PR1, and HSPs associated with plant–pathogen interactions, as well as PALs, CAD, 4CL, CCoAOMT, and CYPs related to phenylpropanoid biosynthesis, were significantly up-regulated in the *MtLOX24*-overexpressing lines. After MeJA treat-

ment, Rboh, CaMCMLs, and CDPKs, which encode pathogen interaction proteins, such as CSE and IFS, which are related to phenylpropanoid synthesis, and the hormone-related JAZ and PP2C were significantly up-regulated in *lox-1*. However, AUX/IAA and PYL4 were significantly up-regulated in the *MtLOX24* overexpression line after MeJA treatment.

Supplementary Materials: The following supporting information can be downloaded at: https://www.mdpi.com/article/10.3390/agriculture14071076/s1, Figure S1: Histogram of GO classification of the annotated unigenes; Figure S2: Heatmap of the expression levels of *MtLOX24* homologous gene before and after MeJA treatment; Table S1: Summary of primer information; Table S2: Quality analysis of the sequence data. Table S3: Summary of GO significant enrichment categories.

Author Contributions: Conceptualization, Q.Y. and R.L.; software, Y.X. (Yanchao Xu), H.L. and Y.X. (Yanran Xu); validation, L.X. and J.K.; formal analysis, M.L.; investigation, L.X. and Y.X. (Yanchao Xu); resources, J.W.; data curation, L.X.; writing—original draft, L.X.; writing—review and editing, R.L.; visualization, Z.L.; supervision, M.L., J.K., Z.L. and R.L.; project administration, Q.Y. and R.L.; funding acquisition, Q.Y. and R.L. All authors have read and agreed to the published version of the manuscript.

Funding: This work was supported by the Key Projects in Science and Technology of Inner Mongolia (2021ZD0031), the Key Research and Development Project of Ningxia Hui Autonomous Region (2022BBF02029), the Agricultural Science and Technology Innovation Program of CAAS (ASTIP-IAS14), and Leading Scientist Project of Gansu Province (23ZDKA013). The funding bodies played no role in the design of this study; the collection, analysis, and interpretation of the data; or the writing of this manuscript.

Institutional Review Board Statement: The data presented in this study are available upon reasonable request from the corresponding author.

Data Availability Statement: The RNA sequencing raw data have been deposited in the Genome Sequence Archive at the National Genomics Data Center, the China National Center for Bioinformation (GSA: CRA017253) and are publicly accessible at https://ngdc.cncb.ac.cn/gsa (accessed on 24 June 2023).

Conflicts of Interest: The authors declare no conflicts of interest.

References

1. Yang, B.; Zhao, Y.; Guo, Z.F. Research Progress and Prospect of Alfalfa Resistance to Pathogens and Pests. *Plants* **2022**, *11*, 2008. [CrossRef]
2. Li, J.; Shang, Q.; Liu, Y.; Dai, W.; Li, X.; Wei, S.; Hu, G.; McNeill, M.R.; Ban, L. Occurrence, Distribution, and Transmission of Alfalfa Viruses in China. *Viruses* **2022**, *14*, 1519. [CrossRef]
3. Howe, G.A.; Major, I.T.; Koo, A.J. Modularity in Jasmonate Signaling for Multistress Resilience. *Annu. Rev. Plant Biol.* **2018**, *69*, 387–415. [CrossRef]
4. Staswick, P.E.; Su, W.; Howell, S.H. Methyl Jasmonate Inhibition of Root Growth and Induction of a Leaf Protein are Decreased in an *Arabidopsis thaliana* mutant. *Proc. Natl. Acad. Sci. USA* **1992**, *89*, 6837–6840. [CrossRef]
5. Hung, K.T.; Kao, C.H. Involvement of Lipid Peroxidation in Methyl Jasmonate-promoted Senescence in Detached Rice Leaves. *Plant Growth Regul.* **1998**, *24*, 17–21. [CrossRef]
6. Wang, F.B.; Wan, C.Z.; Wu, W.Y.; Zhang, Y.N.; Pan, Y.X.; Chen, X.M.; Li, C.; Pi, J.L.; Wang, Z.X.; Ye, Y.X. Methyl Jasmonate (MeJA) Enhances Salt Tolerance of Okra (*Abelmoschus esculentus* L.) Plants by Regulating ABA Signaling, Osmotic Adjustment Substances, Photosynthesis and ROS Metabolism. *Sci. Hortic.* **2023**, *319*, 112145. [CrossRef]
7. Wasternack, C.; Parthier, B. Jasmonate-signalled Plant Gene Expression. *Trends Plant Sci.* **1997**, *2*, 302–307. [CrossRef]
8. Chang, L.J.; Wu, S.; Tian, L. Methyl Jasmonate Elicits Distinctive Hydrolyzable Tannin, Flavonoid, and Phyto-oxylipin Responses in Pomegranate (*Punica granatum* L.) Leaves. *Planta* **2021**, *254*, 89. [CrossRef] [PubMed]
9. Wei, X.B.; Guan, W.L.; Yang, Y.J.; Shao, Y.L.; Mao, L.C. Methyl Jasmonate Promotes Wound Healing by Activation of Phenylpropanoid Metabolism in Harvested Kiwifruit. *Postharvest Biol. Technol.* **2021**, *175*, 111472. [CrossRef]
10. Thaler, J.S.; Stout, M.J.; Karban, R.; Duffey, S.S. Exogenous Jasmonates Simulate Insect Wounding in Tomato Plants (*Lycopersicon esculentum*) in the Laboratory and Field. *J. Chem. Ecol.* **1996**, *22*, 1767. [CrossRef] [PubMed]
11. Chen, Z.; Chen, X.; Yan, H.W.; Li, W.W.; Li, Y.; Cai, R.H.; Xiang, Y. The Lipoxygenase Gene Family in Poplar: Identification, Classification, and Expression in Response to MeJA Treatment. *PLoS ONE* **2015**, *10*, e0125526. [CrossRef] [PubMed]
12. Hu, Z.H.; Zhang, W.; Shen, Y.B.; Fu, H.J.; Su, X.H.; Zhang, Z.Y. Activities of Lipoxygenase and Phenylalanine Ammonia Lyase in Poplar Leaves Induced by Insect Herbivory and Volatiles. *J. For. Res.* **2009**, *20*, 372. [CrossRef]

13. Ogunola, O.F.; Hawkins, L.K.; Mylroie, E.; Kolomiets, M.V.; Borrego, E.; Tang, J.D.; Williams, W.P.; Warburton, M.L. Characterization of the Maize Lipoxygenase Gene Family in Relation to Aflatoxin Accumulation Resistance. *PLoS ONE* **2017**, *12*, e0181265. [CrossRef] [PubMed]
14. Grimes, H.D.; Koetje, D.S.; Franceschi, V.R. Expression, Activity, and Cellular Accumulation of Methyl Jasmonate-responsive Lipoxygenase in Soybean Seedlings. *Plant Physiol.* **1992**, *100*, 433–443. [CrossRef] [PubMed]
15. Hu, T.; Zeng, H.; Hu, Z.L.; Qv, X.X.; Chen, G.P. Overexpression of the Tomato 13-lipoxygenase Gene *TomloxD* Increases Generation of Endogenous Jasmonic Acid and Resistance to *Cladosporium fulvum* and High Temperature. *Plant Mol. Biol. Rep.* **2013**, *31*, 1141–1149. [CrossRef]
16. Yuan, P.G.; Borrego, E.; Park, Y.S.; Gorman, Z.; Huang, P.C.; Tolley, J.; Christensen, S.A.; Blanford, J.; Kilaru, A.; Meeley, R. 9,10-KODA, An α-ketol Produced by the Tonoplast-localized 9-lipoxygenase *ZmLOX5*, Plays a Signaling Role in Maize Defense Against Insect Herbivory. *Mol. Plant* **2023**, *16*, 1283–1303. [CrossRef] [PubMed]
17. Wang, K.D.; Borrego, E.J.; Kenerley, C.M.; Kolomiets, M.V. Oxylipins Other Than Jasmonic Acid Are Xylem-resident Signals Regulating Systemic Resistance Induced by *Trichoderma virens* In Maize. *Plant Cell* **2020**, *32*, 166–185. [CrossRef] [PubMed]
18. Mahgoub, S.; Hashad, N.; Ali, S.; Ibrahim, R.; Said, A.M.; Moharram, F.A.; Mady, M. Polyphenolic Profile of *Callistemon viminalis* Aerial Parts: Antioxidant, Anticancer and In Silico 5-LOX Inhibitory Evaluations. *Molecules* **2021**, *6*, 2481. [CrossRef] [PubMed]
19. Liu, Y.Y.; Du, M.M.; Deng, L.; Shen, J.F.; Fang, M.M.; Chen, Q.; Liu, Y.H.; Wang, Q.M.; Lu, Y.H.; Wang, Q.M.; et al. MYC2 Regulates the Termination of Jasmonate Signaling via an Autoregulatory Negative Feedback Loop. *Plant Cell* **2019**, *31*, 106–127. [CrossRef]
20. Schaller, F. Enzymes of the Biosynthesis of Octadecanoid-derived Signalling Molecules. *J. Exp. Bot.* **2001**, *52*, 11–23. [CrossRef]
21. Xu, L.; Zhu, X.X.; Yi, F.Y.; Liu, Y.J.; Sod, B.; Li, M.N.; Chen, L.; Kang, J.M.; Yang, Q.C.; Long, R.C. A Genome-wide Study of the Lipoxygenase Gene Families in *Medicago truncatula* and *Medicago sativa* Reveals that *MtLOX24* Participates in the Methyl Jasmonate Response. *BMC Genom.* **2024**, *25*, 195. [CrossRef]
22. Chabaud, M.; Ratet, P.; Duque, S.; Araújo, S. Agrobacterium tumefaciens-mediated Transformation and in Vitro Plant Regeneration of *M. truncatula*. In *Medicago truncatula Handbook*; The Samuel Roberts Noble Foundation, Inc.: Ardmore, OK, USA, 2007.
23. Mortazavi, A.; Williams, B.A.; McCue, K.; Schaeffer, L.; Wold, B. Mapping and Quantifying Mammalian Transcriptomes by RNA-Seq. *Nat. Methods* **2008**, *5*, 621–628. [CrossRef]
24. Livak, K.J.; Schmittgen, T.D. Analysis of Relative Gene Expression Data using Real-time Quantitative PCR and the 2(-Delta Delta C(T)) Method. *Methods Companion Methods Enzymol.* **2001**, *4*, 25.
25. Liao, Y.; Smyth, G.K.; Shi, W. featureCounts: An Efficient General Purpose Program for Assigning Sequence Reads to Genomic Features. *Bioinformatics* **2014**, *30*, 923–930. [CrossRef]
26. Bray, N.L.; Pimentel, H.; Páll, M.; Pachter, L. Near-optimal RNA-Seq quantification. *Computer. Sci.* **2015**, *1505*, 02710.
27. Dangl, J.L.; Jones, D.G. Plant Pathogens and Integrated Defence Responses to Infection. *Nature* **2001**, *411*, 826–833. [CrossRef] [PubMed]
28. Farmer, E.E.; Ryan, C.A. Interplant Communication: Airborne Methyl Jasmonate Induces Synthesis of Proteinase Inhibitors in Plant leaves. *Proc. Natl. Acad. Sci. USA* **1990**, *87*, 7713–7716. [CrossRef] [PubMed]
29. Hossain, A.; Pamanick, B.; Venugopalan, V.K.; Ibrahimova, U.; Rahman, M.A.; Siyal, A.L.; Maitra, S.; Chatterjee, S.; Aftab, T. Emerging Roles of Plant Growth Regulators for Plants Adaptation to Abiotic Stress-induced Oxidative Stress. In *Emerging Plant Growth Regulators in Agriculture*; Academic Press: Cambridge, MA, USA, 2022; pp. 1–72.
30. Lang, D.Y.; Yu, X.X.; Jia, X.X.; Li, Z.X.; Zhang, X.H. Methyl Jasmonate Improves Metabolism and Growth of NaCl-stressed *Glycyrrhiza uralensis* Seedlings. *Sci. Hortic.* **2020**, *266*, 109287. [CrossRef]
31. Pan, L.Y.; Zhao, X.Y.; Chen, M.; Fu, Y.Q.; Xiang, M.L.; Chen, J.Y. Effect of Exogenous Methyl Jasmonate Treatment on Disease Resistance of Postharvest Kiwifruit. *Food Chem.* **2020**, *305*, 125483. [CrossRef]
32. Zhu, L.J.; Yu, H.T.; Dai, X.M.; Yu, M.L.; Yu, Z.F. Effect of Methyl Jasmonate on the Quality and Antioxidant Capacity by Modulating Ascorbate-glutathione Cycle in Peach Fruit. *Sci. Hortic.* **2022**, *303*, 111216. [CrossRef]
33. Liao, Z.; Liu, X.; Zheng, J.; Zhao, C.; Wang, D.; Xu, Y.; Sun, C. A Multifunctional True Caffeoyl Coenzyme A O-methyltransferase Enzyme Participates in the Biosynthesis of Polymethoxylated Flavones in Citrus. *Plant Physiol.* **2023**, *192*, 2049–2066. [CrossRef]
34. Barakat, A.; Bagniewska-Zadworna, A.; Choi, A.; Plakkat, U.; DiLoreto, D.S.; Yellanki, P.; Carlson, J.E. The Cinnamyl Alcohol Dehydrogenase Gene Family in Populus: Phylogeny, Organization, and Expression. *BMC Plant Biol.* **2009**, *9*, 26. [CrossRef]
35. Herrero, J.; Carrasco, A.E.; Zapata, J.M. *Arabidopsis thaliana* Peroxidases Involved in Lignin Biosynthesis: In Silico Promoter Analysis and Hormonal Regulation. *Plant Physiol. Biochem.* **2014**, *80*, 192–202. [CrossRef]
36. Naoumkina, M.; Farag, M.A.; Sumner, L.W.; Tang, Y.H.; Liu, C.J.; Dixon, R.A. Different Mechanisms for Phytoalexin Induction by Pathogen and Wound Signals in *Medicago truncatula*. *Proc. Natl. Acad. Sci. USA* **2007**, *104*, 17909–17915. [CrossRef]
37. Yin, Y.Q.; Xue, J.Y.; Hu, J.J.; Yang, Z.F.; Fang, W.M. Exogenous Methyl Jasmonate Combined with Ca^{2+} Promote Resveratrol Biosynthesis and Stabilize Sprout Growth for the Production of Resveratrol-rich Peanut Sprouts. *Plant Physiol. Biochem.* **2023**, *203*, 107988. [CrossRef]
38. Yuan, P.G.; Tanaka, K.; Poovaiah, B.W. Calcium/Calmodulin-mediated Defense Signaling: What Is Looming on the Horizon for AtSR1/CAMTA3-mediated Signaling in Plant Immunity. *Front. Plant Sci.* **2022**, *12*, 795353. [CrossRef]
39. Taga, Y.; Takai, R.; Kaneda, T.; Matsui, H.; Isogai, A.; Che, F.S. Role of *OsHSP90* and IREN, Ca^{2+} Dependent Nuclease, in Plant Hypersensitive Cell Death Induced by Transcription Factor *OsNAC4*. *Plant Signal. Behav.* **2009**, *4*, 740–742. [CrossRef]

40. Chen, J.Y.; Mumtaz, A.; Gonzales-Vigil, E. Evolution and Molecular Basis of Substrate Specificity in A 3-ketoacyl-CoA Synthase Gene Cluster from *Populus trichocarpa*. *J. Biol. Chem.* **2022**, *298*, 102496. [CrossRef]
41. Zhang, H.H.; Wang, F.M.; Song, W.Q.; Yang, Z.H.; Li, L.L.; Ma, Q.; Tan, X.X.; Wei, Z.Y.; Li, Y.J.; Li, J.M. Different Viral Effectors Suppress Hormone-mediated Antiviral Immunity of Rice Coordinated by *OsNPR1*. *Nat. Commun.* **2023**, *14*, 3011. [CrossRef]
42. He, X.; Jiang, J.S.; Wang, C.Q.; Dehesh, K. ORA59 and EIN3 Interaction Couples Jasmonate-ethylene Synergistic Action to Antagonistic Salicylic Acid Regulation of PDF Expression. *J. Integr. Plant Biol.* **2017**, *59*, 275–287. [CrossRef]
43. Guo, H.; Ecker, J.R. Plant Responses to Ethylene Gas are Mediated by SCF(EBF1/EBF2)-dependent Proteolysis of EIN3 Transcription Factor. *Cell* **2003**, *115*, 667–677. [CrossRef]
44. Wang, G.M.; Guo, L.; Guo, Z.H. The Involvement of Ein3-binding F-box protein PbrEBF3 in Regulating Ethylene Signaling during Cuiguan Pear Fruit Ripening. *Plant Sci.* **2023**, *329*, 111600. [CrossRef] [PubMed]
45. Lin, Z.; Li, Y.; Wang, Y.B.; Liu, X.L.; Ma, L.; Zhang, Z.J.; Mu, C.; Zhang, Y.; Peng, L.; Xie, S.J. Initiation and Amplification of SnRK2 Activation in Abscisic Acid Signaling. *Nat. Commun.* **2021**, *12*, 2456. [CrossRef]